



1 **Environmental behaviors of (*E*)-Pyriminobac-methyl in agricultural**
2 **soils**

3

4 Wenwen Zhou^a, Haoran Jia^b, Lang Liu^b, Baotong Li^{b*}, Yuqi Li^b, Meizhu Gao^b

5

6 ^a College of Food Science and Engineering, Jiangxi Agricultural University, Nanchang 330045, China

7 ^b College of Land Resources and Environment, Jiangxi Agricultural University, Nanchang 330045, China

8

9

10

11 *Corresponding Author: Baotong Li, Tel.: 86-791-83813420, E-mail: btli666@163.com



12 **Abstract**

13 (*E*)-Pyriminobac-methyl (EPM), a pyrimidine benzoic acid esters herbicide, has a high potential as
14 weedicide; nevertheless, its environmental behaviors are still not well understood. In this study, we
15 systematically investigated for the first time the adsorption–desorption, degradation, and leaching
16 behaviors of EPM in agricultural soils from five exemplar sites in China (characterized by different
17 physicochemical properties) through laboratory simulation experiments. The EPM adsorption–desorption
18 results were well fitted by the Freundlich model ($R^2 > 0.9999$). In the analyzed soils, the Freundlich
19 adsorption (i.e., K_{f-ads}) and desorption (i.e., K_{f-des}) coefficients of EPM varied between 0.85–32.22 $\text{mg}^{1-1/n}$
20 $\text{L}^{1/n} \text{kg}^{-1}$ and between 0.78–5.02 $\text{mg}^{1-1/n} \text{L}^{1/n} \text{kg}^{-1}$, respectively. Moreover, the degradation of EPM
21 reflected first-order kinetics: its half-life ranged between 37.46–66.00 d depending on the environmental
22 conditions, and abiotic degradation was predominant in the degradation of this compound. The mobility of
23 EPM in the five soils varied from immobile to highly mobile. The groundwater ubiquity score ranged
24 between 0.9765–2.7160, indicating that EPM posed threat to groundwater quality. Overall, the results of
25 this study demonstrate the easy degradability of EPM, as well as its high adsorption affinity and low
26 mobility in soils with abundant organic matter content and high cation exchange capacity. Under such
27 conditions, there is a relatively low contamination risk for groundwater systems in relation to this
28 compound. At the same time, due to its slow degradation, EPM has a low adsorption affinity and tends to
29 be highly mobile in soils poor in organic matter content and with low cation exchange capacity. Under
30 such conditions, there is a relatively high contamination risk for groundwater systems in relation to this
31 compound. Overall, our findings provide a solid basis for predicting the environmental impacts of EPM.

32 **Keywords:** (*E*)-pyriminobac-methyl, adsorption–desorption, degradation, leaching, agricultural soils



33 1. Introduction

34 Herbicides are usually applied to chemically control the growth of weeds associated with different types
35 of crops, both in China and worldwide (Barchanska et al., 2021; Brillas, 2021). Unfortunately, with the
36 applications of weedicides, they have been detected outside of their original application sites, meaning that they
37 contribute to environmental contamination (Jiang et al., 2018; Perotti et al., 2020). In recent years, the
38 groundwater pollution caused by herbicides has attracted increasing attention worldwide (Khan et al., 2020; Wu
39 et al., 2017). Importantly, the environmental fate of herbicides in soil mainly depends on the
40 adsorption–desorption, degradation, and leaching processes. In fact, herbicides can be transferred from soil to
41 groundwater through surface runoff or leaching, resulting in groundwater pollution (Cueff et al., 2020; Gawel et
42 al., 2020). Furthermore, the adsorption–desorption rate and the degradation capability of herbicides regulate the
43 migration of herbicides: the groundwater ubiquity score (GUS) can be used to evaluate their ecological and
44 environmental safety (Acharya et al., 2020; Liu et al., 2021). However, few scholars have assessed the effects of
45 soil properties on the adsorption–desorption, degradation, and leaching behaviors of weedicide, especially the
46 environmental consequences of these changes.

47 Pyriminobac-methyl (PM)[methyl-2-(4,6-dimethoxy-2-pyrimidinylloxy)-6-(1-methoxyiminoethyl) benzoate]
48 (Fig. S1), is composed of a mixture of its (*E*) - isomer (I) and (*Z*) - isomer (II) as the active ingredient due to its
49 chemical structure contain oxime(Song et al., 2010), a mixture of two isomers (I and II) in a > 9:1 (major/minor)
50 ratio which was developed from sulfonylurea by Kumiai Chemical Industry Co., Ltd. In 1996 (Tokyo,
51 Japan)(Tamaru and Saito, 1996). Tamaru et al. (1997)) reported that (*E*) - isomer (I) has been confirmed to
52 restrain the plant enzyme acetolactate synthase (ALS) and prevent branched chain amino acid biosynthesis,
53 and the (*E*) - pyriminobac-methyl (EPM) showed stronger soil adsorption and weaker hydrophilic properties



54 than (Z) - pyriminobac-methyl (ZPM), thus EPM was selected as the best compound to develop a commercial
55 weedicide, which is commonly used to control the growth of sedges and both gramineous and annual weeds.
56 The chemistry of EPM is well understood; the octanol-water partition coefficient is 2.31 (low) at pH 7,
57 20 °C, the solubility - in water is 9.25 mg L⁻¹ (low) at 20 °C, and the vapour pressure is just 3.1×10⁻⁵ Pa
58 (low) at 20 °C (Lewis et al., 2016). A distinct advantage of EPM as a weedicide is that, this compound has
59 an herbicidal activity 1.5–2 times higher and requires an application rate 1/5–1/10 lower than
60 bensulfuron-methyl (a broad-spectrum herbicide) on *Echinochloa crusgalli* and *Leptochloa chinensis* (Iwakami
61 et al., 2015; Shibayama, 2001; Song et al., 2010). Notably, EPM can prevent the growth of *E. crusgalli* and *L.*
62 *chinensis* populations and suppress them effectively over long periods, while being non-toxic, and eventually
63 increasing the yield of paddy rice and subsequent crops (e.g., rape, cabbage, *Astragalus smicus*, wheat, and
64 potato) (Iwafune et al., 2010; Qin et al., 2017; Tang et al., 2010; Yoshii et al., 2020). Nevertheless, few studies
65 have lucubrated the environmental behaviors of EPM after it was widely used as herbicide in the farming
66 industry.

67 Most former investigations on EPM as a weedicide mainly focused on the photo-transformation in water
68 and low temperature storage stability in paddy rice. Inao et al. (2009) demonstrated that the photoconversion of
69 PM in water is the main fate, and the main process is EPM / ZPM reached approximately equilibrium after 4.5 h,
70 furthermore, the EPM / ZPM ratio is about 1/1.35. Another researcher found that even if proper water
71 management to prevent EPM surface runoff from paddy fields was practiced, a significant amount of EPM
72 components were discharged into drainage channels through percolation (Sudo et al., 2018). Nevertheless, the
73 effects of soil properties on the adsorption–desorption, degradation, and leaching behaviors of EPM have rarely
74 been reported.



75 A number of researchers have reported that the soil matrix is a highly complicated system, in which
76 environmental processes (e.g., the sorption–desorption and leaching of herbicides) are affected by multiple
77 factors, including the soil organic matter (OM) content, pH, cation exchange capacity (CEC), microbial or
78 chemical degradation, chemical type, environmental conditions (e.g., temperature, humidity, and rainfall), and
79 texture (Alonso et al., 2011; Rao et al., 2020; Xie et al., 2020; Zhou et al., 2019a). Nevertheless, soil organic
80 or inorganic colloids and pH ($\text{pH} < pK_a$ neutral state and $\text{pH} > pK_a$ negative charge) can influence soil–herbicide
81 interactions. In this context, the leaching of anionic compounds is likely (Pérez-Lucas et al., 2020). Moreover,
82 the leaching of herbicides in soil and the associated risk of water pollution are both affected by sorption and
83 desorption (Xie et al., 2020).

84 Until present, the environmental fate of EPM in soils has not been studied in detail. Clarifying the
85 adsorption and transport of EPM in soil is very important for the protection of surface water and groundwater
86 from EPM pollution. Hence, this study aimed at: 1) gaining an essential understanding of the
87 adsorption–desorption, degradation, and leaching behaviors of EPM in agricultural soils through laboratory
88 simulation experiments; 2) determining the effects of soil properties on the above behaviors in agricultural soils;
89 and 3) conducting a basic evaluation of the safety and applicability of EPM in the environment. Overall, our
90 results provide a scientific basis for the prevention or, at least, minimization of the possible effects of EPM on
91 groundwater, as well as for modeling the fate of EPM in the environment and the potentially associated risks.

92 **2. Materials and Methods**

93 *2.1. Chemicals*



94 EPM (99.0%; chemical formula: $C_{17}H_{19}N_3O_6$; structure shown in Fig. S1) was obtained from ZZBIO Co.,
95 Ltd. (Shanghai, China). Moreover, we used only organic solvents of chromatographic grade (Sigma-Aldrich,
96 Germany). EPM was dissolved in acetonitrile, obtaining a 1000 mg L^{-1} test mother liquor. Moreover, a standard
97 EPM working solution ($0.01\text{--}5.00 \text{ mg L}^{-1}$) was prepared by diluting the stock solution with a CaCl_2 solution
98 (0.01 mol L^{-1}), which was used as an electrolyte to maintain a constant ionic strength and reduce the cationic
99 exchange.

100 In March 2020, five different soils were sampled from the surface layer (0–20 cm) of paddy fields located
101 in five Chinese provinces: Phaeozem (S1, from Heilongjiang), Anthrosol (S2, from Zhejiang), Ferralsol (S3,
102 from Jiangxi), Alisol (S4, from Hubei), and Plinthosol (S5, from Hainan). The soil samples were all air-dried,
103 ground, and passed through a 2-mm sieve before being used. Afterward, standard soil testing methods were
104 applied to define the basic physicochemical properties of the soils (Table S1) (Gee, 1986; Jackson, 1958;
105 Nelson, 1985), which were then classified based on the system of the World Reference Base for Soil Resources
106 (WRB) (L'huillier, 1998). Interestingly, the EPM residues in the analyzed soils were always below the detection
107 limit.

108 2.2. Extraction and final analyses

109 The soil samples were transferred to centrifuge tubes and 10 mL of acetonitrile (containing 0.1% of ammonia
110 water) were added to each of them for extracting EPM. After vortexing the tubes for 5 min, we added 2 g of
111 NaCl and 3 g of MgSO_4 . Then, the tubes were capped and vortexed again for 1 min and centrifuged at $2,400 \times g$
112 for 5 min. The supernatant (1.5 mL) was transferred into a 2.5-mL single-use centrifuge tube that was already
113 containing the sorbent (50 mg C_{18} + 150 mg MgSO_4). Afterward, all the samples were vortexed again for 1 min
114 and centrifuged at 5,000 rpm for 5 min. Finally, the resulting supernatant was extracted with a sterile syringe,



115 passed through a 0.22- μm organic membrane filter, and poured into vials for UPLC system (1260 series, Agilent
116 Technologies, USA) equipped with a triple quadrupole mass spectrometer (6460C series, Agilent Technologies)
117 using positive ion mode in multiple reaction monitoring (MRM) mode analysis. The instrument parameters for
118 Agilent 6460C QQQ UPLC-MS/MS analysis are as follows: The flow rate was maintained at 0.2 mL min⁻¹, and
119 the column (Agilent ZORBAX Eclipse XDB-C18, length 150 mm, inner diameter = 4.6 mm, 5 μm coating) was
120 heated to 35°C. The mobile phase A was water which consisted of 0.1% formate and mobile phase B was
121 acetonitrile. Gradient condition was: 0.0-0.5 min, 20% B; 0.5-1.0 min, 20%-80% B; 1.0-4.0 min, 80% B; 4.0-5.0
122 min, 20% B. The mass spectrometer was operated in electrospray ionization positive with MRM scanning mode,
123 dry gas temperature at 500 °C, Ion source temperature at 150 °C, desolvation gas flow at 1000 L h⁻¹; capillary
124 voltage at 2500 V; cone voltage at 18 V and collision gas was argon, dwell time at 50 ms, collision pressure at
125 58 eV.

126 The efficiency of the EPM extraction during the adsorption–desorption, degradation, and leaching
127 experiments was evaluated based on the results of recovery experiments. The average recovery rates of EPM in
128 the adsorption–desorption experiments, at initial spiked concentrations of 0.1 and 1.0 mg kg⁻¹ in the soils, varied
129 between 94.3–102.4% (relative standard deviation (RSD) = 1.1–3.8%). Meanwhile, the average recovery rates
130 of EPM in soil in the degradation experiments, at initial spiked concentrations of 0.01, 0.2, and 2.0 mg kg⁻¹ in
131 the soils, ranged between 92.6–106.0% (RSD = 1.1–2.9%). Furthermore, the average recovery rates of EPM at
132 initial spiked concentrations of 0.0001, 0.01, and 0.1 mg L⁻¹ in the supernatant of soils were 88.7–107.9% (RSD
133 = 1.7–4.9%). Furthermore, the average recovery rates of EPM in the leaching experiments at initial spiked
134 concentrations of 0.05 and 1.0 mg kg⁻¹ in the soils were 95.8–109% (RSD = 1.6–4.4%).

135 *2.3. Soils samples*



136 The batch equilibration method suggested by the GB 31270.4-2014 guidelines: Adsorption/Desorption in
137 Soils for these soils (Gb, 2014b) was applied to conduct adsorption–desorption experiments. First, for the
138 adsorption kinetics tests, each soil sample (2.0 g) was introduced in a centrifuge tube containing 10 mL of a
139 EPM aqueous solution (1 mg L⁻¹). For each of these tubes, we also analyzed a blank tube (which contained no
140 herbicide) and a control tube (which contained no soil). All the tubes were then shaken by an oscillator at 25 °C
141 ± 1 °C for different time intervals of 0.5, 1, 2, 4, 6, 8, 12, 16, 20, and 24 h.

142 The desorption kinetics were analyzed instead by taking 5 mL of supernatant from each tube after
143 adsorption equilibration and by replacing them with an equal volume of CaCl₂ solution (which contained no
144 EPM). A microvortex mixer was used to thoroughly mix the resulting solution and an oscillator was used to
145 shake it at 25 °C ± 1 °C for several time intervals: 0.5, 1, 2, 4, 6, 8, 12, and 24 h. Finally, for the
146 high-performance liquid chromatography-mass spectrometry (UPLC-MS/MS) analyses, the samples were
147 centrifuged for 10 min at 2,400×g and the supernatants were filtered through 0.22-µm mixed-cellulose ester
148 filter membranes.

149 The adsorption–desorption equilibrium time of EPM in the five soils was 24 h (Fig. 1); moreover, the
150 initial EPM concentrations adopted for these experiments were 0.01, 0.10, 0.50, 1.00, and 5.00 mg L⁻¹. The
151 concentration of EPM in the supernatant was determined after centrifugation. Then, the amount of
152 adsorbed–desorbed EPM in each soil was calculated based on the concentration of EPM in the solution before
153 and after the adsorption–desorption process. The supernatant removed after the adsorption experiments was
154 replaced with 5 mL of CaCl₂ containing no EPM; then, the tubes were shaken for 24 h and centrifuged. Finally,
155 the EPM concentration was determined based on the supernatant collected after this procedure. Considering the



156 results of preliminary experiments and with the aim of desorbing the majority of the adsorbed EPM, we decided
157 to repeat the desorption process for at least three times.

158 *2.4. Degradation experiments*

159 By following the GB 31270.1-2014 guidelines (Gb, 2014c), we performed a series of EPM soil degradation
160 experiments. To ensure aerobic conditions, 20 g of each type of agricultural soil were weighed and introduced
161 in 250-mL Erlenmeyer flasks (in three replicates). Ultrapure water was added during the subsequent cultivation
162 process in order to maintain the soil water content at 60% of the maximum water holding capacity. We then
163 spiked each soil sample with 400 μL of the 100 mg L^{-1} EPM working solution (achieving an initial
164 concentration of 2 mg kg^{-1} in the soil: the water-soluble, organic solvent volume was $\leq 1\%$) and then cultured
165 in the dark in an incubator kept at 25 ± 1 °C. Subsequently, we collected three parallel sub-samples on 0, 1, 2,
166 4, 6, 10, 15, 30, 45, 60, 90, and 120 day, and the EPM content was determined by UPLC-MS/MS on the
167 respective days of collection. The amount of water in the Erlenmeyer flasks was periodically adjusted during
168 the culturing process with the aim of retaining the original water-holding state. Each treatment was done in
169 triplicate, totalizing 60 samples per treatment (5 soil samples per treatment per sampling day; 12 sampling days
170 in total), The following experiment was done in the same way.

171 Another set of experiments was conducted under anaerobic conditions. In this case, we first cultured the
172 soil samples for 30 days and then added a 2 cm-thick water layer to each of them. To maintain the desired
173 conditions, N_2 was continuously introduced into the culture system. The soil samples were subsequently moved
174 into an incubator and cultivated in the dark at 25 ± 1 °C. Finally, three parallel sub-samples were collected on 0,
175 1, 2, 4, 6, 10, 15, 30, 45, 60, 90, and 120 day, and the EPM content was determined by UPLC-MS/MS on the
176 respective days of collection.



177 A set of degradation experiments was performed under sterilized conditions. With this objective, the
178 sterilized soils (20 g each) were weighed and introduced in 250-mL Erlenmeyer flasks in three replicates.
179 Notably, in order to keep the soil water content at 60% of the maximum water holding capacity, sterile water
180 was added during the cultivation process. Then, each soil sample was spiked with 400 μL of the 100 mg L^{-1}
181 EPM working solution, achieving an initial concentration of 2 mg kg^{-1} (the water-soluble, organic solvent
182 volume was $\leq 1\%$). The samples were hence moved into an incubator and cultured in the dark at 25 ± 1 $^{\circ}\text{C}$.
183 Three parallel sub-samples were collected on 0, 1, 2, 4, 6, 10, 15, 30, 45, 60, 90, and 120 day, and the EPM
184 content was determined by UPLC-MS/MS on the respective days of collection.

185 These experiments were done under different soil moisture conditions and aerobic conditions, at a EPM
186 fortification level of 2 mg kg^{-1} . After adjusting their moisture by adding water (water percentage = 40%, 60%,
187 and 80% of the total volume), the soils were incubated in the dark at 25 ± 11 $^{\circ}\text{C}$. During this last phase, we
188 regularly added ultrapure water to keep the moisture at 40%, 60%, and 80%.

189 2.5. Leaching experiments

190 The herbicide leaching process was investigated by following the GB 31270.5-2014 guidelines (Gb, 2014a).
191 PVC columns (length = 35 cm, internal diameter = 4.5 cm), each hand-packed with 600–800 g of one soil type,
192 were used to observe the downward movement of the herbicide. Notably, the top 3 cm and the bottom 2 cm
193 were filled with quartz sand (for minimizing soil disturbance) and glass wool + sea sand (for avoiding soil loss).
194 After packing each column, we removed any air still present in the column by adding 0.01 mol L^{-1} CaCl_2 ;
195 moreover, the excess water was eliminated by gravity. The pore volume (PV) was determined by subtracting the
196 volume of water leached from that of the water added. Subsequently, 1 mL of acetonitrile solution containing
197 200 $\mu\text{g mL}^{-1}$ of the herbicide (spiking level = 1 $\mu\text{g g}^{-1}$) was added to the top of each column. afterward, the



198 adsorption equilibrium was achieved by infiltrating 700 μL of 100 mg L^{-1} EPM solution into soil surface and
199 leaving it to rest for 24 h. To simulate rainfall leaching, 2,000 mL of 0.01 mol L^{-1} CaCl_2 solution (21 mL h^{-1})
200 were added into the soil column at a peristaltic pump speed of 250 mL 12 h^{-1} . The leachate was collected every
201 8 h with a conical flask. Subsequently, each soil column was extracted, cut into three parts (length = 10 cm), and
202 analyzed by UPLC-MS/MS on the same day. The total mass of the leachate and soil fractions along the soil
203 column was determined, together with the EPM and water contents within each of them.

204 2.6. Data analysis

205 The relationship between the concentrations of EPM sorbed in the soil and in the aqueous solution during
206 the sorption–desorption equilibrium was described through the linear [Eq. (1)] and Freundlich [Eq. (2)] models
207 (Azizian et al., 2007; Yang et al., 2021):

$$208 \text{ Linear model: } C_s = KC_e + C \quad (1)$$

$$209 \text{ Freundlich model: } C_s = K_f C_e^{1/n} \quad (2)$$

210 where C_s (mg kg^{-1}) indicates the adsorption of EPM in the soil, C_e (mg L^{-1}) the EPM concentration in the
211 solution during the adsorption equilibrium, C (mg kg^{-1}) the amount of soil adsorption when the EPM
212 concentration was 0 during the adsorption equilibrium, K (mL g^{-1}) and K_f ($\text{mg}^{1-1/n} \text{L}^{1/n} \text{kg}^{-1}$) the
213 adsorption–desorption constants of the linear and Freundlich models, respectively (K_{f-ads}/K_{f-des} in the
214 adsorption–desorption process), and $1/n$ the adsorption empirical constant (which provides information about
215 the non-uniformity of the adsorbent surface).

216 For the isothermal sorption tests, the amount of EPM adsorbed in the soil was estimated using the subtractive
217 method [Eq. (3)]:



$$C_s = \frac{(C_0 - C_e) \times V}{m} \quad (3)$$

218
219 where C_0 (mg L^{-1}) is the amount of soil adsorption when the concentration of EPM was 0 during the adsorption
220 equilibrium, m the soil mass (2.0 g), and V the solution volume (10 mL).

221 The amount of EPM retained by the soil after desorption was obtained instead by using [Eq. (4)], while the
222 hysteresis index (H) was estimated by applying [Eq. (5)] (Fan et al., 2021; Zhang et al., 2020b):

$$C_{si} = \frac{C_0 \times V}{m} - \frac{C_{ej} \times V}{2m} - \frac{V}{m} \sum_{n=1}^j C_e (j-1)$$

$$H = \frac{1/n_{des}}{1/n_{ads}} \quad (5)$$

225 where C_{sj} (mg kg^{-1}) is the concentration of EPM adsorbed by the soil after the j -th desorption ($i = 1-5$), C_{ej}
226 (mg L^{-1}) the EPM concentration in the supernatant after the j -th desorption, H the hysteresis coefficient, and
227 $1/n_{ads}$ and $1/n_{des}$ the empirical adsorption and desorption constants, respectively.

228 The distribution coefficient (K_d) was calculated based on the distribution ratio of EPM in the water–soil
229 system by using [Eq. (6)] (Carballa et al., 2008; Ternes et al., 2004):

$$K_d = \frac{C_s}{C_e} \quad (6)$$

230
231 The sorption constants of the OC (K_{OC}) and OM (K_{OM}) contents were calculated through [Eqs. (7) and (8)]
232 (Rae et al., 1998; Zhang et al., 2011), respectively. Moreover, the Gibbs free energy change of sorption (ΔG , kJ
233 mol^{-1}) (Jia et al., 2019) and the GUS (Gustafson, 1989) were calculated as follows:



$$234 \quad K_{OM} = 100 \times K_{f-ads} / OM\% \quad (7)$$

$$235 \quad K_{OC} = 100 \times K_d / OC\% \quad (8)$$

$$236 \quad \Delta G = -RT \ln K_{OM} / 1000 \quad (9)$$

$$237 \quad GUS = \lg t_{1/2} \times (4 - \lg K_{OC}) \quad (10)$$

238 where OM % and OC % represent the soil OM and OC contents, respectively, R the molar gas constant
239 ($8.314 \text{ J K}^{-1} \text{ mol}^{-1}$), T (K) the absolute temperature, and $t_{1/2}$ the half-life (in days) given by [Eq. (12)]. Organic
240 contaminants were categorized into five types: highly adsorbed compounds ($K_{OC} > 20,000$), sub-highly adsorbed
241 compounds ($5,000 < K_{OC} \leq 20,000$), medium-adsorbed compounds ($1,000 < K_{OC} \leq 5,000$), sub-difficultly
242 adsorbed compounds ($200 < K_{OC} \leq 1,000$), and difficultly adsorbed compounds ($K_{OC} \leq 200$)(Gb, 2014b).

243 The degradation data relative to herbicides in soil could be successfully fitted to a first-order kinetic model
244 [Eq. (11)], previously used in similar studies (Bailey et al., 1968; Liu et al., 2021; Ou et al., 2020):

$$245 \quad C_t = C_0 e^{-kt} \quad (11)$$

246 where C_t (mg kg^{-1}) and C_0 (mg kg^{-1}) are the concentrations of EPM in the soil at incubation times t (d) and
247 0 (d), respectively, while k is the first-order rate constant (d^{-1}).

248 The half-life ($t_{1/2}$) to be used in above model was calculated through [Eq. (12)] (Yin and Zelenay, 2018):

$$249 \quad t_{1/2} = 0.693/k \quad (12)$$

250 Four categories of herbicide degradability were defined: easily degradable ($t_{1/2} \leq 30$), moderately
251 degradable ($30 < t_{1/2} \leq 90$), slightly degradable ($90 < t_{1/2} \leq 180$), and poorly degradable ($t_{1/2} > 180$)(Gb, 2014c).



252 Based on the content of EPM in different sections of the soil columns and in the leachate [Eq. (13)](Gb,
253 2014a), we were able to calculate the leaching rate of EPM:

$$254 \quad R_i = \frac{m_i}{m_0} \times 100 \quad (13)$$

255 where R_i (%) is the ratio of EPM content in each soil section or in the leachate to the total added amount, m_i
256 (mg) the mass of EPM in each soil section (where $i = 1, 2, 3$, and 4, representing the 0–10 cm, 10–20 cm, and
257 20–30 cm soil sections and in the leachate, respectively), and m_0 (mg) the total added amount of EPM ($m_0 =$
258 0.02 mg). Regarding the mobility scheme we defined the following R_i ranges: class 1 (immobile, $R_1 > 50$ %),
259 class 2 (slightly mobile, $R_2 + R_3 + R_4 > 50$ %), class 3 (mobile, $R_3 + R_4 > 50$ %), and class 4 (highly mobile,
260 $R_4 > 50$ %)(Gb, 2014a).

261 The data fittings (to the linear and Freundlich models for the adsorption isotherms and to the simple
262 first-order kinetic model for degradation) were conducted with OriginPro 8.05 (OriginLab Corp., Northampton,
263 USA). All the values reported here were calculated as the means of three replicates; furthermore, the differences
264 between these means were statistically analyzed through Duncan's multiple range test, while their reciprocal
265 relationships were determined through a Spearman's correlation analysis using SPSS Statistics 22.0 (IBM SPSS,
266 Somers, USA).

267 3. Results and discussion

268 3.1. Adsorption–desorption kinetics

269 The adsorption and desorption kinetic curves of EPM in different types of agricultural soils are shown in
270 Fig. 1. After EPM had been in contact with the soil solution for 1 h, the concentration of EPM exhibited a sharp
271 drop (from 0 to 95.35, 75.45, 51.57, 77.41 and finally 65.84 % between S1–S5). This event corresponded to the



272 fast sorption phase. After 2–8 h, the EPM soil system entered the slow adsorption stage and there was a gradual
273 increase in the sorption of EPM. This last process reached an equilibrium state of EPM sorption after 8 h, which
274 was reflected by stable concentrations of EPM. The sorption of EPM decreased from the Phaeozem (S1, 97.99%)
275 to the Anthrosol (S2, 79.69%), Alisol (S4, 77.81%), Plinthosol (S5, 72.57%), and Ferralsol (S3, 52.35%) (Fig.
276 1a). This trend reflected the soils' OM contents. Previous studies have also found that the sorption of organic
277 chemicals in soils is mainly related to their OM contents (Xu et al., 2021; Zhou et al., 2019b).

278 The desorption equilibration of EPM in soil was slightly slower and a hysteresis effect was observed. The
279 rapid and slow desorption stages occurred between 0–2 h and 2–12 h, respectively; afterward, the concentration
280 of EPM remained unchanged, until the desorption process reached its equilibrium state (within 24 h). Based on
281 these data, we defined 24 h as the period of EPM adsorption-desorption. The desorption value of EPM observed
282 in our experiments after 24 h increased from the Phaeozem (S1, 8.04%) to the Anthrosol (S2, 12.07%), Alisol
283 (S4, 14.48%), Plinthosol (S5, 17.55%), and Ferralsol (S3, 24.08%) (Fig. 1b).

284 The sorption of OM in soil typically occurs during the rapid reaction and slow equilibrium phases (Calvet,
285 1989). Therefore, the reduction of the EPM content in the solution before and after the experiment was likely
286 due to soil sorption. According to the above results, the soil sorption rate was inversely proportional to the soil
287 desorption rate toward EPM.

288 3.2. Adsorption–desorption isotherms

289 Non-linear adsorption–desorption isotherms of EPM were observed (Fig. 1). When the concentration of
290 EPM was low, this compound was preferentially adsorbed by OM (which has a strong adsorption capacity);
291 meanwhile, soils with higher OM contents (e.g., Phaeozems, S1) desorbed EPM slowly. The positive



292 relationship between sorption and OM has been reported previously (Hochman et al., 2021; Obregón
293 Alvarez et al., 2021; Patel et al., 2021). Moreover, the adsorption ability of EPM has been found to be high,
294 similar to those of other herbicides (e.g., chlorsulfuron, imazamethabenz-methyl, flumetsulam, and
295 bispyribac-sodium) (Kalsi and Kaur, 2019; Medo et al., 2020; Spadotto et al., 2020). Generally, a low
296 mobility of herbicides in soil is related to a high sorption constant. Hence, the EPM contained in the soils
297 tested in this study (excluding the phaeozem, S1) is likely to have been polluting the groundwater and
298 surface water of the respective areas of origin.

299 OM adsorption in soil is currently explained mainly by partitioning and adsorption-site theories (Martins and
300 Mermoud, 1998), which are well described by the linear and Freundlich isotherm models, respectively. Our
301 isothermal sorption and desorption data were thus fitted to these two models: the obtained fitting parameters are
302 listed in Table 1. The average R^2 value for the linear model (0.9950) was smaller than that for the Freundlich
303 model (0.9999); moreover, the C values obtained for the Plinthosol (S5, -0.01 ± 0.06) by fitting the data to the
304 linear model were negative (Table 1) and did not meet the experimental requirements, indicating that this type of
305 model was not suitable for this experiment. Meanwhile, the sorption-site theory was found to more accurately
306 describe the sorption–desorption process: the Freundlich model provided a more accurate description of the
307 EPM sorption-desorption characteristics observed in this study.

308 Generally, larger K_{f-ads} values correspond to higher sorption capacities (Carneiro et al., 2020; Khorram et al.,
309 2018; Silva et al., 2019). Here, the K_{f-ads} values of EPM ranged between 0.85 (in S4) and 32.22 (in S1) ($\text{mg}^{1-1/n}$
310 $\text{L}^{1/n} \text{kg}^{-1}$), while the $1/n_{f-ads}$ values ranged between 0.80 (S1) and 1.06 (S5) (Table 1). In brief, S5 showed an
311 S-type adsorption isotherm (since $1/n_{f-ads} > 1$), while S1, S2, S3, and S4 showed an L-type adsorption isotherm
312 (since $1/n_{f-ads} < 1$). In this study, the H values of EPM ranged between 0.013 (Phaeozem, S1) and 0.845



313 (Ferralsol, S3). Since the H values were < 0.7 in S1, S2, S4, and S5, these particular soils showed a positive
314 hysteresis: the desorption rate of EPM was lower than its sorption rate. Meanwhile, since the H values in S3
315 were between 0.7–1.0, the sorption and desorption rates were in equilibrium: S3 did not exhibit any obvious
316 hysteresis. Similar results were reported that hysteresis was absent when $0.7 < H < 1$ (Gao and Jiang, 2010; Yue
317 et al., 2017; Barriuso et al., 1994).

318 Soil physicochemical properties are important factors influencing herbicide adsorption behaviors (Urach
319 Ferreira et al., 2020; Wei et al., 2020). We determined the relationship between the Freundlich
320 adsorption–desorption constant and the soil physicochemical (soil pH, CEC, soil clay content, OM content, and
321 OC content) properties and carried out a linear correlation analysis based on the experimental data fitting (Table
322 S2). The results showed that the soil pH, CEC, soil clay content, OM content, and OC content were positively
323 correlated with K_{f-des} and K_{f-ads} (slope > 0). In soils, some polar contents, ionizable groups, and the CEC tend to
324 increase during OM humification (Calvet, 1989; Meimaroglou and Mouzakis, 2019; Rae et al., 1998). This
325 mechanism possibly explains the adsorption of EPM in soils high in OM and CEC. Our findings agree with
326 those of Acharya et al. (2020) and García-Delgado et al. (2020): the soil humic acid and clay fractions (high in
327 OM and CEC and possessing a high number of active sites) are capable of intense EPM adsorption; in contrast,
328 the soil coarse sand fraction (low in OM and CEC) is characterized by a weaker EPM adsorption. Notably, the
329 soil with the highest fumigant adsorption capacity was also possibly that with the highest OM abundance and
330 CEC. For example, strong linear and positive correlations have been found between the adsorption–desorption
331 of benzobicyclon hydrolysate and the soil clay content, OC content, OM content, and CEC, while moderate
332 linear and negative correlations were observed between those processes and the soil pH (Rao et al., 2020).



333 The K_{OC} value is typically used to indicate the EPM sorption capacity of a soil (Fao, 2000; Xiang, 2019)
334 (see Table 2). EPM was sub-difficultly adsorbed in S2, S3, S4, and S5: this aspect was reflected by the K_{OC}
335 values, which ranged between 200–1,000. However, in S1 the K_{OC} values ranged between 1,000–5,000,
336 indicating a medium adsorbance of EPM in this soil. Overall, an increasing trend in the mobility of EPM was
337 observed from the Phaeozem (S1) to the Anthrosol (S2), Alisol (S4), Plinthosol (S5), and Ferralsol (S3). We
338 hence infer that a relatively low soil adsorption capacity is linked to a relatively high mobility of EPM in that
339 soil.

340 The degree of spontaneity of the adsorption process can be quantitatively evaluated based on variations in
341 the ΔG values: negative ΔG values generally indicate that an adsorption process is spontaneous and exothermic
342 (Nandi et al., 2009). Notably, the change of free energy linked to physical adsorption is smaller than that linked
343 to chemisorption. The former is in the range of -20 to 0 kJ mol^{-1} , while the latter is in the range of -80 to -400
344 kJ mol^{-1} (Bulut and Aydın, 2006; Yu et al., 2004). We found that the ΔG values relative to EPM adsorption in all
345 soils were comprised between -16.2242 and -12.5753 kJ mol^{-1} . Therefore, the adsorptions we observed in our
346 experiments can be regarded as typically spontaneous and exothermic physical adsorptions (Table 2).

347 3.3. Degradation of EPM in soil

348 To investigate the effects of aerobic and anaerobic microorganisms on EPM degradation, we sterilized the soil
349 samples or removed all aerobic microorganisms. The soil samples were kept in the dark at 25 °C, maintaining a
350 soil moisture of 60%. The degradation kinetics of EPM under aerobic, anaerobic, and sterilized conditions are
351 depicted in Fig. 2, while the fitted parameters are summarized in Table 3. The R^2 values for EPM in the five
352 soils ranged between 0.9313–0.9924, suggesting that the first-order kinetic model agreed with the
353 correspondent degradation data. The half-life of EPM ranged between 37.46–58.25 d in the aerobic soils,



354 between 41.75–59.74 d in the anaerobic soils, and between 60.87–66.00 d in the sterilized soils. A moderate
355 degradation ($30 \text{ d} < t_{1/2} \leq 90 \text{ d}$) of EPM was observed under aerobic, anaerobic, and sterilized conditions. These
356 results can be partly explained by aerobic and anaerobic transformations occurring in the soils, which have been
357 described by the GB 31270.1-2014 guidelines for the testing of chemicals (Gb, 2014c). Overall, the half-life of
358 EPM decreased from the aerobic to the anaerobic and sterilized soils. Understanding the degradation kinetics of
359 herbicides is critical for predicting their persistence in soil and the soil parameters, which affect regional
360 agronomic and environmental practices (Buerge et al., 2019; Buttiglieri et al., 2009). Under dark conditions, the
361 degradation of herbicides in soil mainly results from microbial and abiotic degradation (Marín-Benito et al.,
362 2019). In this study, when EPM was retained under dark conditions for 30 d, its degradation rates in all soils
363 under sterilized conditions (35.44, 36.27, 33.27, 32.80, and 34.78%) were a little slower than under anaerobic
364 (48.60, 41.51, 35.92, 35.61, and 38.07%) and aerobic conditions (53.32, 43.20, 36.73, 35.61, and 39.31%) (Fig.
365 2). As the degradation rate increased only by 10% compared to that observed under sterilized conditions,
366 degradation under aerobic/anaerobic conditions appeared to be mainly abiotic degradation. In contrast, other
367 studies have found that anaerobic microorganisms are predominant contributors in the degradation process and
368 capable of accelerating it. For example, the degradation rates of phenazine-1-carboxamide (PCN) were much
369 higher under anaerobic than aerobic conditions, due to its own structural characteristics (Ou et al., 2020).
370 Between 30–120 d, there were no significant differences in the degradation rates of EPM between sterilized and
371 unsterilized soils, suggesting that EPM degradation was largely abiotic in this time interval. This might be
372 attributed to a low bioavailability of EPM for microbial degradation, derived from a high adsorption affinity of
373 this compound under the right OM content and pH conditions (Liu et al., 2021; Wang et al., 2020a). Overall, it
374 appears that EPM decomposition in the tested soils was mainly driven by abiotic degradation.



375 The degradation rate of EPM decreased from S1 to S2, S4, S5, and S3 under both aerobic and anaerobic
376 conditions (Table 3). A negative correlation was noted between the half-life of EPM and the soil OM content
377 and CEC under aerobic conditions (slope < 0, $P < 0.05$; $R^2 = 0.9478$ and 0.8022 , respectively); besides, a
378 negative correlation was observed between the half-life of EPM and the soil OM content under aerobic
379 conditions (slope < 0, $P < 0.05$, $R^2 = 0.8983$). Notably, an abundance of OM and high CEC result in an increase
380 of the carbon sources accessible to microorganisms, effectively stimulating their activity (Xu et al., 2020). In the
381 presence of microorganisms, the particularly high OM and CEC characterizing S1, resulted in the fastest EPM
382 degradation among those observed in all soils under aerobic and anaerobic conditions. However, under sterilized
383 conditions, the degradation rate of EPM decreased from S2 to S4, S1, S5, and S3 (Table 3); moreover, the
384 half-life of EPM and the soil pH exhibited a negative correlation under these same conditions (slope < 0, $P <$
385 0.05 , $R^2 = 0.8850$; Table S3). The rate of EPM hydrolysis is known to be positively affected by alkaline soil pH.
386 This relationship explains why, in the presence of elevated hydrolysis and under sterilized conditions, the fastest
387 degradation behavior among all the tested soils was observed in S2 (which was characterized by the highest pH).
388 Notably, the highest differences in the degradation rate of EPM were observed under aerobic conditions. In
389 order to comprehensively evaluate the influence of various factors on this degradation rate, we hence focused on
390 the analysis of data collected under aerobic conditions.

391 The data regarding the degradation behavior of EPM in the tested soils (Table 4 and Fig. 2) conform to
392 first-order kinetics ($R^2 > 0.8769$). The half-life of EPM varied depending on the moisture conditions: it
393 diminished from soils with a 60% moisture to those with moisture of 80% and 40%. Additionally, after 120 days,
394 the degradation rates of EPM in soils with a 40% moisture (74.59, 73.93, 69.98, 73.21, and 71.25 for S1–S5,
395 respectively) were obviously lower than those in soils with 80% (77.55, 75.38, 72.79, 75.44, and 73.62 for



396 S1–S5, respectively) and 60% (80.04, 77.31, 75.43, 77.78, and 75.77% for S1–S5, respectively) moistures
397 (Table 4 and Fig. 2d, e). These results show that, when the soil moisture increased from 40% to 60%, the decay
398 rate of EPM accelerated, possibly due to the stimulation of a degradation pathway (e.g., through aerobic
399 microorganisms and chemical hydrolysis) linked to the increase in soil moisture (Wang et al., 2014; Liu et al.,
400 2021). Conversely, EPM showed a slower decay when the soil moisture increased from 60% to 80%. This
401 phenomenon might have been caused by an increase in sorption, which would have made EPM less bioavailable.
402 This effect was more or less important according to the predominance of different biotic pathways of
403 degradation (Bento et al., 2016; García-Valcárcel and Tadeo, 1999).

404 *3.4. Leaching potential*

405 In the current study, leaching experiments were performed by using soil columns, with the aim of
406 simulating the migration of EPM in several agricultural soils. The correspondent results are shown in Fig. 3. It
407 was found that the fluidity of EPM was lower in S₁ than in S₂, S₃, S₄, or S₅. Furthermore, the R_i values of this
408 compound in S₁, S₂, S₃, S₄, and S₅ were R₁ = 99 %, R₂ + R₃ + R₄ = 55.5 %, R₄ = 71.95 %, R₂ + R₃ + R₄ = 76 %,
409 and R₂ + R₃ + R₄ = 74 %, respectively. Based on the Test guidelines on environmental safety assessment for
410 chemical pesticide-Part 5: Leaching in soil (Gb, 2014a), the mobility of EPM in the soils S1–S5 was categorized
411 as immobile, slightly mobile, highly mobile, slightly mobile, and slightly mobile, respectively. The soil OM
412 content was found to be the most important soil property influencing the mobility of molecular herbicides,
413 followed by the clay content and the CEC. A lower clay content is usually associated with a higher sand content,
414 a higher proportion of large pores, a smaller specific surface area per soil unit volume, and a lower adsorption
415 affinity for herbicides, which, overall, result in a greater herbicide mobility (Boyd et al., 1988; De Matos et al.,
416 2001; Kulshrestha et al., 2004; Temminghoff et al., 1997). We found that a lower soil OM content corresponded



417 to a weaker adsorption affinity, a weaker tendency of EPM to pass from the soil solution to the solid phase, a
418 higher availability of EPM for leaching, and a stronger mobility of this same compound. Notably, the OM
419 content increased from the Ferralsol (S3) to the Plinthosol (S5), Alisol (S4), Anthrosol (S2), and Phaeozems
420 (S1), while the mobility of EPM increased from the Phaeozem (S1) to the Anthrosol (S2), Alisol (S4), Plinthosol
421 (S5), and Ferralsol (S3). This mobility tendency is the opposite compared to the adsorption affinity tendency of
422 EPM in the five soils. As a matter of fact, it is generally known that the mobility of EPM in soil increases as its
423 adsorption affinity decreases. Similar conclusions were reached through the study of other herbicides (Acharya
424 et al., 2020; Zhang et al., 2020a).

425 Here, the GUS was also used to estimate both the leaching potential of chemicals and the risk of
426 contaminants into groundwater. The GUS values of EPM in S1, S2, S3, S4, and S5 were 0.9765, 2.0402, 2.7160,
427 2.3755, and 2.6765, respectively (Table 2). The GUS value in S1 was considerably lower than 1.8, EPM should
428 have little leaching potential in this soil (Gustafson, 1989; Wang et al., 2020b); meanwhile, since the GUS
429 values in the S2, S3, S4, and S5 soils were between 1.8–2.8, EPM has a considerable leaching potential there
430 and, possibly, the ability to pollute groundwater (Huang, 2019; Martins et al., 2018). Overall, we can infer that
431 the risk of groundwater contamination by EPM is low in Phaeozem (S1), due to the low mobility of this
432 compound; however, the risk is much higher when the same compound is contained in Anthrosol (S2), Ferralsol
433 (S3), Alisol (S4), and Plinthosol (S5).

434 **4. Conclusions**

435 In this study, we found that EPM degrades easily, has a high adsorption affinity and a low mobility in Phaeozem
436 (S1), which result in a low contamination risk for groundwater systems. On the contrary, this compound
437 degrades slowly in Anthrosol (S2), Ferralsol (S3), Alisol (S4), and Plinthosol (S5), due to a low adsorption



438 affinity and moderate mobility, which result in a high contamination risk for groundwater systems. The
439 adsorption–desorption, degradation, and leaching of EPM were systematically explored in five agricultural soils.
440 We noticed that physical adsorption was the main mode of EPM adsorption. The effects of soil physicochemical
441 properties on the adsorption and desorption of this compound were quantified by linear regression analysis. In
442 this regard, the Freundlich adsorption (K_{f-ads}) and desorption (K_{f-des}) constants were linearly and positively
443 correlated with the soil OC content, OM content, and CEC, while nonsignificant correlations were observed
444 among the above constants and the soil pH and clay content.

445 The dissipation of EPM depended mainly on soil conditions (i.e., moisture, pH, and soil type). EPM
446 degradation was most likely derived from abiotic degradation mechanisms; furthermore, the leaching ability of
447 EPM increased from the Phaeozem (S1) to the Anthrosol (S2), Alisol (S4), Plinthosol (S5), and Ferralsol (S3).
448 Overall, the high leaching ability and desorption capacity of EPM were accompanied by a low adsorption
449 capacity and there were no significant relationships between pH and the leaching rate of EPM in the five types
450 of soils. In contrast, the OM content, CEC, and soil clay content were the main responsible for the observed
451 leaching rates.

452 To completely understand the fate of EPM in the environment, it is necessary to perform additional studies
453 on the microbial community structures and functional diversities of other types of soil besides those analyzed
454 here. As a matter of fact, there are still only a few studies on the environmental fate of EPM; therefore, our
455 results may serve as a reference for evaluating the risks involved in the increasingly wide application of this
456 compound.

457 **Declaration of Competing Interest**



458 The authors declare that they have no known competing financial interests or personal relationships that
459 could have appeared to influence the work reported in this paper.

460 **Acknowledgements**

461 This work is financially supported by the National Key Research and Development Plan of China
462 (2017YFD0301604).

463 **References**

- 464 Acharya, S. P., Johnson, J., and Weidhaas, J.: Adsorption kinetics of the herbicide safeners, benoxacor and
465 furilazole, to activated carbon and agricultural soils, *Journal of Environmental Sciences*, 89, 23-34,
466 <https://doi.org/10.1016/j.jes.2019.09.022>, 2020.
- 467 Alonso, D. G., Koskinen, W. C., Oliveira, R. S., Constantin, J., and Mislankar, S.: Sorption–Desorption of
468 Indaziflam in Selected Agricultural Soils, *J Agric Food Chem*, 59, 13096-13101, 10.1021/jf203014g, 2011.
- 469 Azizian, S., Haerifar, M., and Basiri-Parsa, J.: Extended geometric method: A simple approach to derive
470 adsorption rate constants of Langmuir–Freundlich kinetics, *Chemosphere*, 68, 2040-2046,
471 <https://doi.org/10.1016/j.chemosphere.2007.02.042>, 2007.
- 472 Bailey, G. W., White, J. L., and Rothberg, T.: Adsorption of Organic Herbicides by Montmorillonite: Role of pH
473 and Chemical Character of Adsorbate, 32, 222-234,
474 <https://doi.org/10.2136/sssaj1968.03615995003200020021x>, 1968.
- 475 Barchanska, H., Tang, J., Fang, X., Danek, M., Płonka, J., and Sajdak, M.: Profiling and fingerprinting strategies to
476 assess exposure of edible plants to herbicides, *Food Chemistry*, 335, 127658,
477 <https://doi.org/10.1016/j.foodchem.2020.127658>, 2021.
- 478 Barriuso, E., Laird, D., Koskinen, W., and Dowdy, R.: Atrazine Desorption From Smectites, *Soil Science Society of
479 America Journal - SSSAJ*, 58, 10.2136/sssaj1994.03615995005800060008x, 1994.
- 480 Bento, C. P. M., Yang, X., Gort, G., Xue, S., van Dam, R., Zomer, P., Mol, H. G. J., Ritsema, C. J., and Geissen, V.:
481 Persistence of glyphosate and aminomethylphosphonic acid in loess soil under different combinations of
482 temperature, soil moisture and light/darkness, *Science of The Total Environment*, 572, 301-311,
483 <https://doi.org/10.1016/j.scitotenv.2016.07.215>, 2016.
- 484 Boyd, S. A., Lee, J.-F., and Mortland, M. M.: Attenuating organic contaminant mobility by soil modification,
485 *Nature*, 333, 345-347, 10.1038/333345a0, 1988.
- 486 Brillas, E.: Recent development of electrochemical advanced oxidation of herbicides. A review on its application
487 to wastewater treatment and soil remediation, *Journal of Cleaner Production*, 290, 125841,
488 <https://doi.org/10.1016/j.jclepro.2021.125841>, 2021.
- 489 Buerge, I. J., Bächli, A., Kasteel, R., Portmann, R., López-Cabeza, R., Schwab, L. F., and Poiger, T.: Behavior of the
490 Chiral Herbicide Imazamox in Soils: pH-Dependent, Enantioselective Degradation, Formation and Degradation
491 of Several Chiral Metabolites, *Environmental Science & Technology*, 53, 5725-5732, 10.1021/acs.est.8b07209,
492 2019.



- 493 Bulut, Y. and Aydin, H.: A kinetics and thermodynamics study of methylene blue adsorption on wheat shells,
494 Desalination, 194, 259-267, <https://doi.org/10.1016/j.desal.2005.10.032>, 2006.
- 495 Buttiglieri, G., Peschka, M., Frömel, T., Müller, J., Malpei, F., Seel, P., and Knepper, T. P.: Environmental
496 occurrence and degradation of the herbicide n-chloridazon, Water Research, 43, 2865-2873,
497 <https://doi.org/10.1016/j.watres.2009.03.035>, 2009.
- 498 Calvet, R.: Adsorption of organic chemicals in soils, Environmental Health Perspectives, 83, 145-177, 1989.
- 499 Carballa, M., Fink, G., Omil, F., Lema, J. M., and Ternes, T.: Determination of the solid-water distribution
500 coefficient (Kd) for pharmaceuticals, estrogens and musk fragrances in digested sludge, Water Research, 42,
501 287-295, <https://doi.org/10.1016/j.watres.2007.07.012>, 2008.
- 502 Carneiro, G. D. O. P., Souza, M. d. F., Lins, H. A., Chagas, P. S. F. d., Silva, T. S., Teófilo, T. M. d. S., Pavão, Q. S.,
503 Grangeiro, L. C., and Silva, D. V.: Herbicide mixtures affect adsorption processes in soils under sugarcane
504 cultivation, Geoderma, 379, 114626, <https://doi.org/10.1016/j.geoderma.2020.114626>, 2020.
- 505 Cueff, S., Alletto, L., Dumény, V., Benoit, P., and Pot, V.: Adsorption and degradation of the herbicide
506 nicosulfuron in a stagnic Luvisol and Vermic Umbrisol cultivated under conventional or conservation agriculture,
507 Environmental Science and Pollution Research, 10.1007/s11356-020-11772-2, 2020.
- 508 de Matos, A. T., Fontes, M. P. F., da Costa, L. M., and Martinez, M. A.: Mobility of heavy metals as related to soil
509 chemical and mineralogical characteristics of Brazilian soils, Environmental Pollution, 111, 429-435,
510 [https://doi.org/10.1016/S0269-7491\(00\)00088-9](https://doi.org/10.1016/S0269-7491(00)00088-9), 2001.
- 511 Fan, X., Zou, Y., Geng, N., Liu, J., Hou, J., Li, D., Yang, C., and Li, Y.: Investigation on the adsorption and
512 desorption behaviors of antibiotics by degradable MPs with or without UV ageing process, Journal of
513 Hazardous Materials, 401, 123363, <https://doi.org/10.1016/j.jhazmat.2020.123363>, 2021.
- 514 FAO: Assessing soil contamination A reference manual, Parameters of pesticides that influence processes in the
515 soil, FOOD AND AGRICULTURE ORGANIZATION OF THE UNITED NATIONS Rome, Rome2000.
- 516 Gao, H.-J. and Jiang, X.: Effect of Initial Concentration on Adsorption-Desorption Characteristics and Desorption
517 Hysteresis of Hexachlorobenzene in Soils, Pedosphere, 20, 104-110,
518 [https://doi.org/10.1016/S1002-0160\(09\)60289-7](https://doi.org/10.1016/S1002-0160(09)60289-7), 2010.
- 519 García-Delgado, C., Marín-Benito, J. M., Sánchez-Martín, M. J., and Rodríguez-Cruz, M. S.: Organic carbon
520 nature determines the capacity of organic amendments to adsorb pesticides in soil, Journal of Hazardous
521 Materials, 390, 122162, <https://doi.org/10.1016/j.jhazmat.2020.122162>, 2020.
- 522 García-Valcárcel, A. I. and Tadeo, J. L.: Influence of Soil Moisture on Sorption and Degradation of Hexazinone
523 and Simazine in Soil, J Agric Food Chem, 47, 3895-3900, 10.1021/jf981326i, 1999.
- 524 Gawel, A., Seiwert, B., Sühnhholz, S., Schmitt-Jansen, M., and Mackenzie, K.: In-situ treatment of
525 herbicide-contaminated groundwater-Feasibility study for the cases atrazine and bromacil using two novel
526 nanoremediation-type materials, Journal of Hazardous Materials, 393, 122470,
527 <https://doi.org/10.1016/j.jhazmat.2020.122470>, 2020.
- 528 GB: Test Guidelines on Environmental Safety Assessment for Chemical Pesticides: Part 5: Leaching in soil,
529 2014a.
- 530 GB: Test Guidelines of the Environmental Safety Assessment for Chemical Pesticides-Part 4:
531 Adsorption/Desorption in Soils, 2014b.
- 532 GB: Test Guidelines of the Environmental Safety Assessment for Chemical Pesticides-Part 1 (Transformation in
533 Soils) 2014c.
- 534 Gee, G. W., and Bauder, J. W. : 'Particle-size analysis' in Methods of soil analysis, part-I. Physical and
535 mineralogical methods, Madison, WI: American Society of Agronomy and Soil Science Society of America,



- 536 1986.
- 537 Gustafson, D. I.: Groundwater ubiquity score: A simple method for assessing pesticide leachability,
538 Environmental Toxicology and Chemistry, 8, 339-357, 10.1002/etc.5620080411, 1989.
- 539 Hochman, D., Dor, M., and Mishael, Y.: Diverse effects of wetting and drying cycles on soil aggregation:
540 Implications on pesticide leaching, Chemosphere, 263, 127910,
541 <https://doi.org/10.1016/j.chemosphere.2020.127910>, 2021.
- 542 Huang, B., Yan, D. D., Wang, X. N., Wang, X. L., Fang, W.S., Zhang, D. Q., Ouyang, C. B., Wang, Qi. X., Cao, A. C.:
543 Soil fumigation alters adsorption and degradation behavior of pesticides in soil, Environmental Pollution, 246,
544 264-273, <https://doi.org/10.1016/j.envpol.2018.12.003>, 2019.
- 545 Inao, K., Mizutani, H., Yogo, Y., and Ikeda, M.: Improved PADDY model including photoisomerization and
546 metabolic pathways for predicting pesticide behavior in paddy fields: Application to the herbicide
547 pyriminobac-methyl, Journal of Pesticide Science, advpub, 0909190094-0909190094, 10.1584/jpestics.G09-20,
548 2009.
- 549 Iwafune, T., Inao, K., Horio, T., Iwasaki, N., Yokoyama, A., and Nagai, T.: Behavior of paddy pesticides and major
550 metabolites in the Sakura River, Ibaraki, Japan, Journal of Pesticide Science, advpub, 1001130109-1001130109,
551 10.1584/jpestics.G09-49, 2010.
- 552 Iwakami, S., Hashimoto, M., Matsushima, K.-i., Watanabe, H., Hamamura, K., and Uchino, A.:
553 Multiple-herbicide resistance in Echinochloa crus-galli var. formosensis, an allohexaploid weed species, in
554 dry-seeded rice, Pesticide Biochemistry and Physiology, 119, 1-8, <https://doi.org/10.1016/j.pestbp.2015.02.007>,
555 2015.
- 556 Jackson, M.: Soil Chemical Analysis, prentice Hall. Inc, Englewood Cliffs, NJ, 1958.
- 557 Jia, C.-S., Zhang, L.-H., Peng, X.-L., Luo, J.-X., Zhao, Y.-L., Liu, J.-Y., Guo, J.-J., and Tang, L.-D.: Prediction of entropy
558 and Gibbs free energy for nitrogen, Chemical Engineering Science, 202, 70-74,
559 <https://doi.org/10.1016/j.ces.2019.03.033>, 2019.
- 560 Jiang, R., Wang, M., Chen, W., and Li, X.: Ecological risk evaluation of combined pollution of herbicide siduron
561 and heavy metals in soils, Science of The Total Environment, 626, 1047-1056,
562 <https://doi.org/10.1016/j.scitotenv.2018.01.135>, 2018.
- 563 Kalsi, N. K. and Kaur, P.: Dissipation of bispyribac sodium in aridisols: Impact of soil type, moisture and
564 temperature, Ecotoxicology and Environmental Safety, 170, 375-382,
565 <https://doi.org/10.1016/j.ecoenv.2018.12.005>, 2019.
- 566 Khan, M. A., Costa, F. B., Fenton, O., Jordan, P., Fennell, C., and Mellander, P.-E.: Using a multi-dimensional
567 approach for catchment scale herbicide pollution assessments, Science of The Total Environment, 747, 141232,
568 <https://doi.org/10.1016/j.scitotenv.2020.141232>, 2020.
- 569 Khorram, M. S., Sarmah, A. K., and Yu, Y.: The Effects of Biochar Properties on Fomesafen
570 Adsorption-Desorption Capacity of Biochar-Amended Soil, Water, Air, & Soil Pollution, 229, 60,
571 10.1007/s11270-017-3603-2, 2018.
- 572 Kulshrestha, P., Giese, R. F., and Aga, D. S.: Investigating the Molecular Interactions of Oxytetracycline in Clay
573 and Organic Matter: Insights on Factors Affecting Its Mobility in Soil, Environmental Science & Technology, 38,
574 4097-4105, 10.1021/es034856q, 2004.
- 575 L'Huillier, L., Dupont, S., Dubus, I., Becquer, T., Bourdon, E.: Carence et fixation du phosphore dans les sols
576 ferrallitiques ferritiques de Nouvelle-Caledonie, XVIe Congres Mondial de Science du Sol, Montpellier, France,
577 20-26 1998.
- 578 Lewis, K. A., Tzilivakis, J., Warner, D. J., and Green, A.: An international database for pesticide risk assessments



- 579 and management, *Human and Ecological Risk Assessment: An International Journal*, 22, 1050-1064,
580 10.1080/10807039.2015.1133242, 2016.
- 581 Liu, J., Zhou, J. H., Guo, Q. N., Ma, L. Y., and Yang, H.: Physicochemical assessment of environmental behaviors of
582 herbicide atrazine in soils associated with its degradation and bioavailability to weeds, *Chemosphere*, 262,
583 127830, <https://doi.org/10.1016/j.chemosphere.2020.127830>, 2021.
- 584 Marín-Benito, J. M., Carpio, M. J., Sánchez-Martín, M. J., and Rodríguez-Cruz, M. S.: Previous degradation study
585 of two herbicides to simulate their fate in a sandy loam soil: Effect of the temperature and the organic
586 amendments, *Science of The Total Environment*, 653, 1301-1310,
587 <https://doi.org/10.1016/j.scitotenv.2018.11.015>, 2019.
- 588 Martins, E. C., de Freitas Melo, V., Bohone, J. B., and Abate, G.: Sorption and desorption of atrazine on soils:
589 The effect of different soil fractions, *Geoderma*, 322, 131-139,
590 <https://doi.org/10.1016/j.geoderma.2018.02.028>, 2018.
- 591 Martins, J. M. and Mermoud, A.: Sorption and degradation of four nitroaromatic herbicides in mono and
592 multi-solute saturated/unsaturated soil batch systems, *J Contam Hydrol*, 33, 187-210,
593 [https://doi.org/10.1016/S0169-7722\(98\)00070-9](https://doi.org/10.1016/S0169-7722(98)00070-9), 1998.
- 594 Medo, J., Hricáková, N., Maková, J., Medová, J., Omelka, R., and Javoreková, S.: Effects of sulfonyleurea
595 herbicides chlorsulfuron and sulfosulfuron on enzymatic activities and microbial communities in two
596 agricultural soils, *Environmental Science and Pollution Research*, 27, 41265-41278,
597 10.1007/s11356-020-10063-0, 2020.
- 598 Meimaroglou, N. and Mouzakis, C.: Cation Exchange Capacity (CEC), texture, consistency and organic matter in
599 soil assessment for earth construction: The case of earth mortars, *Construction and Building Materials*, 221,
600 27-39, <https://doi.org/10.1016/j.conbuildmat.2019.06.036>, 2019.
- 601 Nandi, B. K., Goswami, A., and Purkait, M. K.: Adsorption characteristics of brilliant green dye on kaolin, *Journal*
602 *of Hazardous Materials*, 161, 387-395, <https://doi.org/10.1016/j.jhazmat.2008.03.110>, 2009.
- 603 Nelson, D., Sommers, L., : Total carbon, organic carbon and organic matter. , In *Methods of Soil Analysis*,
604 American Society of Agronomy, USA1985.
- 605 Obregón Alvarez, D., Mendes, K. F., Tosi, M., Fonseca de Souza, L., Campos Cedano, J. C., de Souza Falcão, N. P.,
606 Dunfield, K., Tsai, S. M., and Tornisiello, V. L.: Sorption-desorption and biodegradation of sulfometuron-methyl
607 and its effects on the bacterial communities in Amazonian soils amended with aged biochar, *Ecotoxicology and*
608 *Environmental Safety*, 207, 111222, <https://doi.org/10.1016/j.ecoenv.2020.111222>, 2021.
- 609 Ou, J., Li, H., Ou, X., Yang, Z., Chen, M., Liu, K., Teng, Y., and Xing, B.: Degradation, adsorption and leaching of
610 phenazine-1-carboxamide in agricultural soils, *Ecotoxicology and Environmental Safety*, 205, 111374,
611 <https://doi.org/10.1016/j.ecoenv.2020.111374>, 2020.
- 612 Patel, K. F., Tejnecký, V., Ohno, T., Bailey, V. L., Sleighter, R. L., and Hatcher, P. G.: Reactive oxygen species alter
613 chemical composition and adsorptive fractionation of soil-derived organic matter, *Geoderma*, 384, 114805,
614 <https://doi.org/10.1016/j.geoderma.2020.114805>, 2021.
- 615 Pérez-Lucas, G., Gambín, M., and Navarro, S.: Leaching behaviour appraisal of eight persistent herbicides on a
616 loam soil amended with different composted organic wastes using screening indices, *Journal of Environmental*
617 *Management*, 273, 111179, <https://doi.org/10.1016/j.jenvman.2020.111179>, 2020.
- 618 Perotti, V. E., Larran, A. S., Palmieri, V. E., Martinatto, A. K., and Permingeat, H. R.: Herbicide resistant weeds: A
619 call to integrate conventional agricultural practices, molecular biology knowledge and new technologies, *Plant*
620 *Science*, 290, 110255, <https://doi.org/10.1016/j.plantsci.2019.110255>, 2020.
- 621 Qin, M., Chai, S., Ma, Y., Gao, H., Zhang, H., and He, Q.: Determination of pyriminobac-methyl and



- 622 bispyribac-sodium residues in rice by liquid chromatography-tandem mass spectrometry based on QuEChERS,
623 *Se pu = Chinese journal of chromatography*, 35, 719-723, 10.3724/sp.J.1123.2017.02032, 2017.
- 624 Rae, J. E., Cooper, C. S., Parker, A., and Peters, A.: Pesticide sorption onto aquifer sediments, *Journal of*
625 *Geochemical Exploration*, 64, 263-276, [https://doi.org/10.1016/S0375-6742\(98\)00037-5](https://doi.org/10.1016/S0375-6742(98)00037-5), 1998.
- 626 Rao, L., Luo, J., Zhou, W., Zou, Z., Tang, L., and Li, B.: Adsorption-desorption behavior of benzobicyclon
627 hydrolysate in different agricultural soils in China, *Ecotoxicology and Environmental Safety*, 202, 110915,
628 <https://doi.org/10.1016/j.ecoenv.2020.110915>, 2020.
- 629 Shibayama, H.: Weeds and weed management in rice production in Japan, *Weed Biology and Management*, 1,
630 53-60, <https://doi.org/10.1046/j.1445-6664.2001.00004.x>, 2001.
- 631 Silva, T. S., de Freitas Souza, M., Maria da Silva Teófilo, T., Silva dos Santos, M., Formiga Porto, M. A., Martins
632 Souza, C. M., Barbosa dos Santos, J., and Silva, D. V.: Use of neural networks to estimate the sorption and
633 desorption coefficients of herbicides: A case study of diuron, hexazinone, and sulfometuron-methyl in Brazil,
634 *Chemosphere*, 236, 124333, <https://doi.org/10.1016/j.chemosphere.2019.07.064>, 2019.
- 635 Song, H., Mao, H., and Shi, D.: Synthesis and Herbicidal Activity of α -Hydroxy Phosphonate Derivatives
636 Containing Pyrimidine Moiety, 28, 2020-2024, <https://doi.org/10.1002/cjoc.201090337>, 2010.
- 637 Spadotto, C. A., Locke, M. A., Bingner, R. L., and Mingoti, R.: Estimating sorption of monovalent acidic
638 herbicides at different pH levels using a single sorption coefficient, *Pest Management Science*, 76, 2693-2698,
639 <https://doi.org/10.1002/ps.5815>, 2020.
- 640 Sudo, M., Goto, Y., Iwama, K., and Hida, Y.: Herbicide discharge from rice paddy fields by surface runoff and
641 percolation flow: A case study in paddy fields in the Lake Biwa basin, Japan, *Journal of Pesticide Science*, 43,
642 24-32, 10.1584/jpestics.D17-061, 2018.
- 643 Tamaru, M. and Saito, Y.: Studies of the New Herbicide KIH-6127. Part I. Novel Synthesis of Methyl
644 6-Acetylsalicylate as a Key Synthetic Intermediate for the Preparation of 6-Acetyl Pyrimidin-2-yl Salicylates and
645 Analogues, *Pesticide Science*, 47, 125-130,
646 [https://doi.org/10.1002/\(SICI\)1096-9063\(199606\)47:2<125::AID-PS394>3.0.CO;2-X](https://doi.org/10.1002/(SICI)1096-9063(199606)47:2<125::AID-PS394>3.0.CO;2-X), 1996.
- 647 Tamaru, M., Masuyama, N., Sato, M., Takabe, F., Inoue, J., and Hanai, R.: Studies of the New Herbicide KIH-6127.
648 Part III. Synthesis and Structure-Activity Studies of Analogues of KIH-6127 against Barnyard Grass (*Echinochloa*
649 *oryzicola*)*, *Pesticide Science*, 49, 76-84,
650 [https://doi.org/10.1002/\(SICI\)1096-9063\(199701\)49:1<76::AID-PS491>3.0.CO;2-E](https://doi.org/10.1002/(SICI)1096-9063(199701)49:1<76::AID-PS491>3.0.CO;2-E), 1997.
- 651 Tang, W., Yu, Z.-H., and Shi, D.-Q.: Synthesis, crystal structure, and herbicidal activity of pyrimidinyl benzylamine
652 analogues containing a phosphonyl group, *Heteroatom Chemistry*, 21, 148-155,
653 <https://doi.org/10.1002/hc.20589>, 2010.
- 654 Temminghoff, E. J. M., Van der Zee, S. E. A. T. M., and de Haan, F. A. M.: Copper Mobility in a
655 Copper-Contaminated Sandy Soil as Affected by pH and Solid and Dissolved Organic Matter, *Environmental*
656 *Science & Technology*, 31, 1109-1115, 10.1021/es9606236, 1997.
- 657 Ternes, T. A., Herrmann, N., Bonerz, M., Knacker, T., Siegrist, H., and Joss, A.: A rapid method to measure the
658 solid-water distribution coefficient (Kd) for pharmaceuticals and musk fragrances in sewage sludge, *Water*
659 *Research*, 38, 4075-4084, <https://doi.org/10.1016/j.watres.2004.07.015>, 2004.
- 660 Urach Ferreira, P. H., Ferguson, J. C., Reynolds, D. B., Kruger, G. R., and Irby, J. T.: Droplet size and
661 physicochemical property effects on herbicide efficacy of pre-emergence herbicides in soybean (*Glycine max* (L.)
662 Merr), 76, 737-746, <https://doi.org/10.1002/ps.5573>, 2020.
- 663 Wang, H. Z., Zuo, H. G., Ding, Y. J., Miao, S. S., Jiang, C., and Yang, H.: Biotic and abiotic degradation of pesticide
664 Dufulin in soils, *Environmental Science and Pollution Research*, 21, 4331-4342, 10.1007/s11356-013-2380-8,



- 665 2014.
- 666 Wang, Q., Fu, Y., Zhang, L., Ling, S., and Wu, Y.: Determination of pyriminobac-methyl isomers in paddy and its
667 storage stability, *Journal of Food Safety and Quality*, 20, 7429-7435, 2020a.
- 668 Wang, Z., Yang, L., Cheng, P., Yu, Y., Zhang, Z., and Li, H.: Adsorption, degradation and leaching migration
669 characteristics of chlorothalonil in different soils, *European Journal of Remote Sensing*, 1-10,
670 10.1080/22797254.2020.1771216, 2020b.
- 671 Wei, L., Huang, Y., Huang, L., Li, Y., Huang, Q., Xu, G., Müller, K., Wang, H., Ok, Y. S., and Liu, Z.: The ratio of H/C
672 is a useful parameter to predict adsorption of the herbicide metolachlor to biochars, *Environmental Research*,
673 184, 109324, <https://doi.org/10.1016/j.envres.2020.109324>, 2020.
- 674 Wu, X., Wang, W., Liu, J., Pan, D., Tu, X., Lv, P., Wang, Y., Cao, H., Wang, Y., and Hua, R.: Rapid Biodegradation of
675 the Herbicide 2,4-Dichlorophenoxyacetic Acid by *Cupriavidus gilardii* T-1, *J Agric Food Chem*, 65, 3711-3720,
676 10.1021/acs.jafc.7b00544, 2017.
- 677 Xiang, L., Wang, X. D., Chen, X. H., Mo, C. H., Li, Y. W., Li, H., Cai, Q. Y., Zhou, D. M., Wong, M. H., Li, Q. X.:
678 Sorption Mechanism, Kinetics, and Isotherms of Di-n-butyl Phthalate to Different Soil Particle-Size Fractions, *J*
679 *Agric Food Chem*, 67, 4734-4745, 10.1021/acs.jafc.8b06357, 2019.
- 680 Xie, G., Li, B., Tang, L., Rao, L., and Dong, Z.: Adsorption-desorption and leaching behaviors of broflanilide in
681 four texturally different agricultural soils from China, *Journal of Soils and Sediments*,
682 10.1007/s11368-020-02831-9, 2020.
- 683 Xu, Y., Yu, X., Xu, B., Peng, D., and Guo, X.: Sorption of pharmaceuticals and personal care products on soil and
684 soil components: Influencing factors and mechanisms, *Science of The Total Environment*, 753, 141891,
685 <https://doi.org/10.1016/j.scitotenv.2020.141891>, 2021.
- 686 Xu, Y., Liu, J., Cai, W., Feng, J., Lu, Z., Wang, H., Franks, A. E., Tang, C., He, Y., and Xu, J.: Dynamic processes in
687 conjunction with microbial response to disclose the biochar effect on pentachlorophenol degradation under
688 both aerobic and anaerobic conditions, *Journal of Hazardous Materials*, 384, 121503,
689 <https://doi.org/10.1016/j.jhazmat.2019.121503>, 2020.
- 690 Yang, R., Jia, A., He, S., Hu, Q., Sun, M., Dong, T., Hou, Y., and Zhou, S.: Experimental investigation of water
691 vapor adsorption isotherm on gas-producing Longmaxi shale: Mathematical modeling and implication for water
692 distribution in shale reservoirs, *Chemical Engineering Journal*, 406, 125982,
693 <https://doi.org/10.1016/j.cej.2020.125982>, 2021.
- 694 Yin, X. and Zelenay, P.: (Invited) Kinetic Models for the Degradation Mechanisms of PGM-Free ORR Catalysts,
695 *ECS Transactions*, 85, 1239-1250, 10.1149/08513.1239ecst, 2018.
- 696 Yoshii, K., Okada, M., Tsumura, Y., Nakamura, Y., Ishimtsu, S., and Tonogai, Y.: Supercritical Fluid Extraction of
697 Ten Chloracetanilide Pesticides and Pyriminobac-Methyl in Crops: Comparison with the Japanese Bulletin
698 Method, *Journal of AOAC INTERNATIONAL*, 82, 1239-1245, 10.1093/jaoac/82.5.1239 %J *Journal of AOAC*
699 *INTERNATIONAL*, 2020.
- 700 Yu, Y., Zhuang, Y.-Y., Wang, Z.-H., and Qiu, M.-Q.: Adsorption of water-soluble dyes onto modified resin,
701 *Chemosphere*, 54, 425-430, [https://doi.org/10.1016/S0045-6535\(03\)00654-4](https://doi.org/10.1016/S0045-6535(03)00654-4), 2004.
- 702 Yue, L., Ge, C., Feng, D., Yu, H., Deng, H., and Fu, B.: Adsorption-desorption behavior of atrazine on agricultural
703 soils in China, *Journal of Environmental Sciences*, 7, 180-189, 2017.
- 704 Zhang, C.-L., Qiao, G.-L., Zhao, F., and Wang, Y.: Thermodynamic and kinetic parameters of ciprofloxacin
705 adsorption onto modified coal fly ash from aqueous solution, *Journal of Molecular Liquids*, 163, 53-56,
706 <https://doi.org/10.1016/j.molliq.2011.07.005>, 2011.
- 707 Zhang, S., Han, B., Sun, Y., and Wang, F.: Microplastics influence the adsorption and desorption characteristics



708 of Cd in an agricultural soil, *Journal of Hazardous Materials*, 388, 121775,
709 <https://doi.org/10.1016/j.jhazmat.2019.121775>, 2020a.

710 Zhang, Y., Li, W., Zhou, W., Jia, H., and Li, B.: Adsorption-desorption characteristics of pyraclonil in eight
711 agricultural soils, *Journal of Soils and Sediments*, 20, 1404-1412, 10.1007/s11368-019-02471-8, 2020b.

712 Zhou, W., Zhang, Y., Li, W., Jia, H., Huang, H., and Li, B.: Adsorption isotherms, degradation kinetics, and
713 leaching behaviors of cyanogen and hydrogen cyanide in eight texturally different agricultural soils from China,
714 *Ecotoxicology and Environmental Safety*, 185, 109704, <https://doi.org/10.1016/j.ecoenv.2019.109704>, 2019a.

715 Zhou, Z., Yan, T., Zhu, Q., Bu, X., Chen, B., Xue, J., and Wu, Y.: Bacterial community structure shifts induced by
716 biochar amendment to karst calcareous soil in southwestern areas of China, *Journal of Soils and Sediments*, 19,
717 356-365, 10.1007/s11368-018-2035-y, 2019b.

718

719

720

721

722

723

724



725

726 **Table 1**

727 Comparison between the results of the linear and Freundlich models for the adsorption–desorption of EPM in five agricultural soils.

Soil sample	Soil type	Adsorption				Desorption							
		Linear model		Freundlich model		Linear model		Freundlich model					
		K (mL g ⁻¹) ^a	C_0 (mg kg ⁻¹) ^a	R^2	$K_{f,ads}$ (mg ¹⁻ⁿ L ^{1/n} kg ⁻¹) ^a	$1/n_{ads}$ ^a	R^2	K (mL g ⁻¹) ^a	R^2	K_{f-des} (mg ¹⁻ⁿ L ^{1/n} kg ⁻¹) ^a	$1/n_{des}$ ^a	R^2	H
S1	Phaeozem	56.21 ± 3.56	0.17 ± 0.01	0.9841	32.22 ± 4.55	0.80 ± 0.07	0.9999	0.80 ± 0.24	0.8384	5.02 ± 0.02	0.01 ± 33.53	0.9999	0.013
S2	Anthrosol	2.78 ± 0.06	0.13 ± 0.04	0.9982	2.95 ± 0.04	0.88 ± 0.03	0.9999	0.27 ± 0.03	0.9823	2.27 ± 0.01	0.71 ± 0.28	0.9999	0.807
S3	Ferralsol	2.43 ± 0.07	0.16 ± 0.05	0.9975	2.65 ± 0.03	0.84 ± 0.03	0.9999	0.82 ± 0.19	0.8988	1.73 ± 0.05	0.11 ± 1.43	0.9999	0.131
S4	Alisol	0.79 ± 0.01	0.05 ± 0.01	0.9990	0.85 ± 0.02	0.95 ± 0.03	0.9999	0.53 ± 0.05	0.9834	0.78 ± 0.01	0.12 ± 0.01	1.0000	0.126
S5	Plinthosol	2.03 ± 0.07	-0.01 ± 0.06	0.9951	1.99 ± 0.05	1.06 ± 0.04	0.9999	2.53 ± 0.18	0.9905	1.38 ± 0.08	0.19 ± 0.56	0.9999	0.179

728 ^a The values represent means ± standard error (SE, n = 3).



729 **Table 2**

730 Empirical constants, Gibbs free energy, and groundwater ubiquity score (GUS) for the adsorption of EPM
731 in five agricultural soils.

Soil sample	Soil type	K	C _e /C ₀	K _{f,ads} (mg ^{1-1/n} L ^{1/n} kg ⁻¹)	K _{OC}	K _{OM}	ΔG (kJ mol ⁻¹)	GUS
S1	Phaeozem	64.4821	0.0117	32.2230	2395.8435	695.6897	-16.2242	0.9765
S2	Anthrosol	3.0971	0.2441	2.9540	606.7513	335.2273	-14.4143	2.0402
S3	Ferralsol	2.7861	0.2641	2.6530	289.3500	159.6386	-12.5753	2.7160
S4	Alisol	0.8393	0.5437	0.8520	413.3906	242.8571	-13.6153	2.3755
S5	Plinthosol	2.0172	0.3314	1.9950	289.8034	165.8333	-12.6696	2.6765

732

733

734

735

736

737

738

739

740

741

742

743

744

745

746

747

748



749 **Table 3**

750 Degradation kinetic models and parameters of EPM under different conditions.

Soil sample	Soil type	Aerobic			Anaerobic			Sterilized		
		First-order kinetic model	Half-life $t_{1/2}$ (d)	R^2	First-order kinetic model	Half-life $t_{1/2}$ (d)	R^2	First-order kinetic model	Half-life $t_{1/2}$ (d)	R^2
S1	Phaeozem	$C_1 = 1.5338e^{-0.0185t}$	37.46	0.9473	$C_1 = 1.7792e^{-0.0166t}$	41.75	0.9579	$C_1 = 1.8467e^{-0.0111t}$	62.43	0.9800
S2	Anthrosol	$C_1 = 1.6419e^{-0.0146t}$	47.47	0.9707	$C_1 = 1.8599e^{-0.0139t}$	49.85	0.9696	$C_1 = 1.7543e^{-0.0113t}$	60.87	0.9551
S3	Ferralsol	$C_1 = 1.9363e^{-0.0119t}$	58.25	0.9843	$C_1 = 1.9968e^{-0.0116t}$	59.74	0.9878	$C_1 = 1.9349e^{-0.0105t}$	66.00	0.9775
S4	Alisol	$C_1 = 1.9476e^{-0.0133t}$	52.10	0.9924	$C_1 = 1.9477e^{-0.0133t}$	52.11	0.9924	$C_1 = 1.7086e^{-0.0112t}$	61.88	0.9313
S5	Plinthosol	$C_1 = 1.7864e^{-0.0126t}$	55.00	0.9655	$C_1 = 1.9725e^{-0.0121t}$	57.27	0.9923	$C_1 = 1.8638e^{-0.0109t}$	63.58	0.9761

751

752

753

754

755

756

757

758



759

760 **Table 4**

761 Degradation kinetic models and parameters of EPM in soil under different moisture conditions.

Soil sample	Soil type ^a	Saturation moisture capacity (40%)			Saturation moisture capacity (60%)			Saturation moisture capacity (80%)		
		First-order kinetic model	Half-life $t_{1/2}$ (d)	R^2	First-order kinetic model	Half-life $t_{1/2}$ (d)	R^2	First-order kinetic model	Half-life $t_{1/2}$ (d)	R^2
S1	Phaeozem	$C_1 = 1.7324e^{-0.0141t}$	49.15	0.9582	$C_1 = 1.5338e^{-0.0185t}$	37.46	0.9473	$C_1 = 1.7792e^{-0.0166t}$	41.75	0.9579
S2	Anthrosol	$C_1 = 1.6551e^{-0.0133t}$	52.11	0.8769	$C_1 = 1.6419e^{-0.0146t}$	47.47	0.9707	$C_1 = 1.8599e^{-0.0139t}$	49.87	0.9696
S3	Ferralsol	$C_1 = 1.8659e^{-0.0110t}$	62.77	0.9884	$C_1 = 1.9363e^{-0.0119t}$	58.25	0.9843	$C_1 = 1.9968e^{-0.0116t}$	59.74	0.9878
S4	Alisol	$C_1 = 1.8428e^{-0.0116t}$	59.74	0.9742	$C_1 = 1.9476e^{-0.0133t}$	52.10	0.9924	$C_1 = 1.7076e^{-0.0121t}$	57.27	0.9849
S5	Plinthosol	$C_1 = 1.7637e^{-0.0104t}$	66.63	0.9650	$C_1 = 1.7864e^{-0.0126t}$	55.00	0.9655	$C_1 = 1.9725e^{-0.0121t}$	57.27	0.9923

762

763

764

765

766

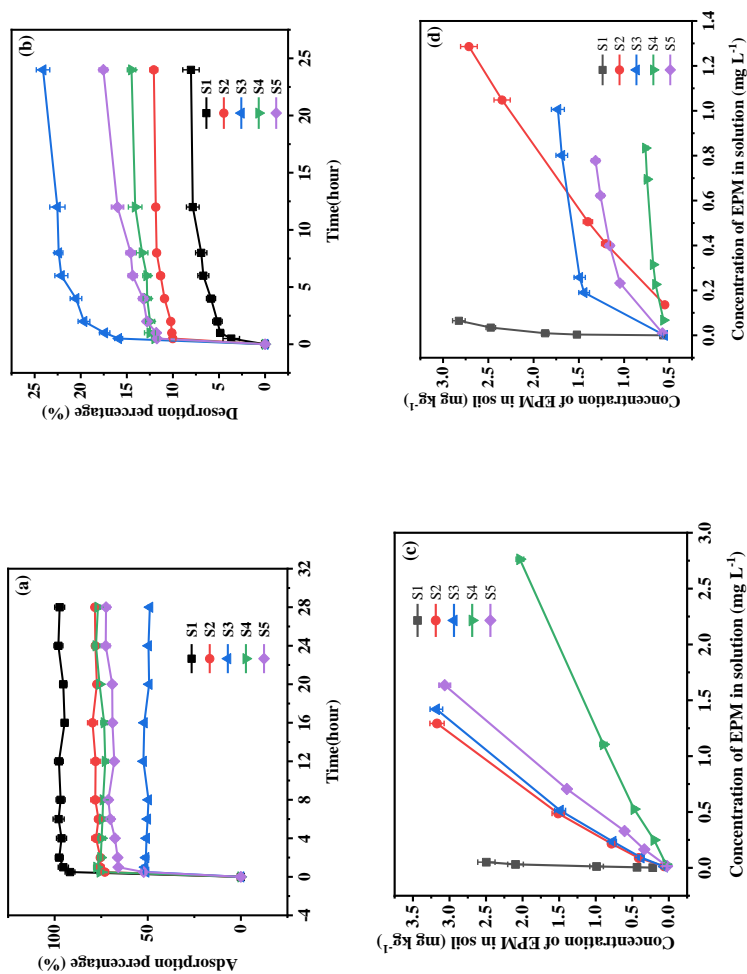
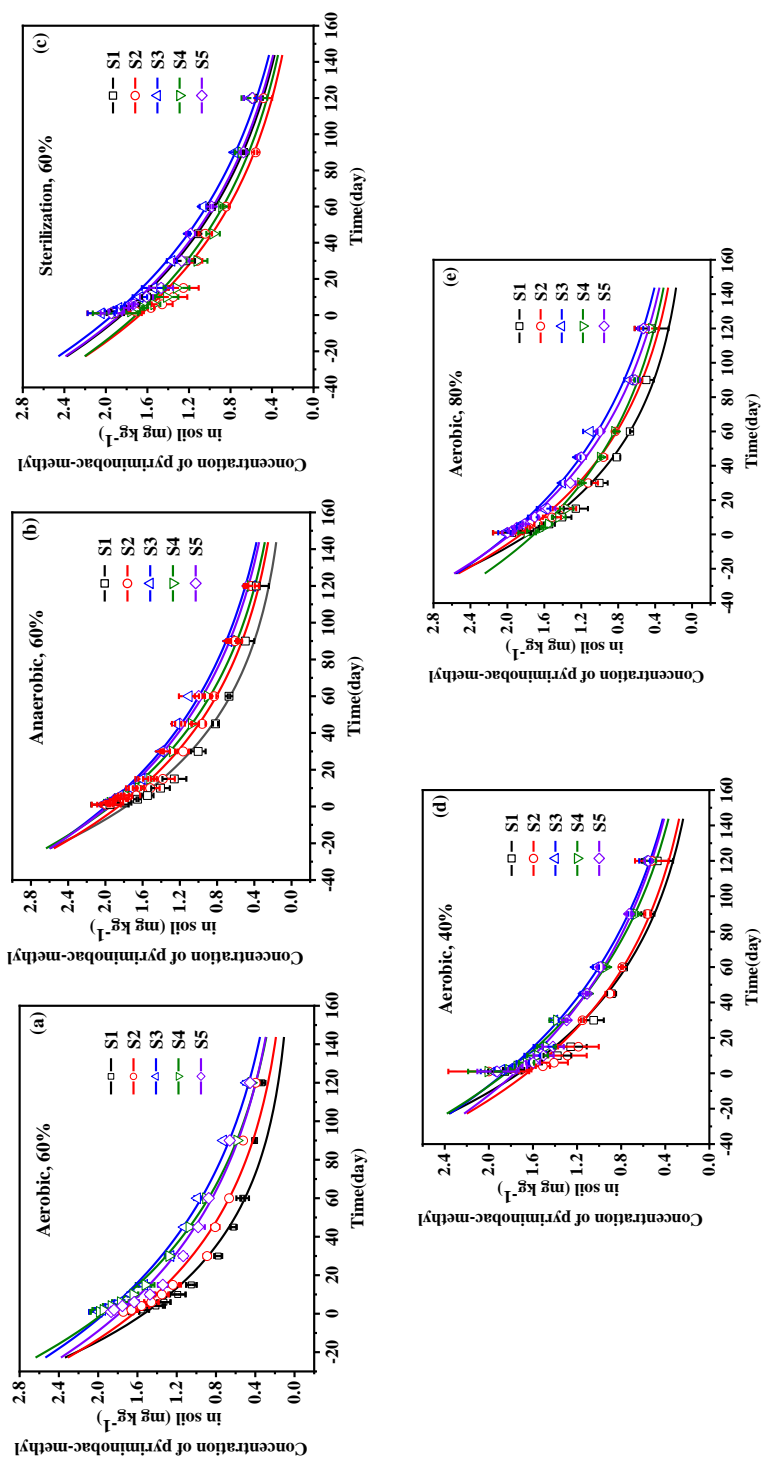


Fig. 1 Adsorption (a) and desorption (b) kinetic curves and Adsorption (c) and desorption (d) isothermal curves of EPM in five different agricultural soils (S1 to S5 are defined in Table 1). Values are the means \pm standard error (n=3).



771
 772
 773 **Fig. 2** Degradation kinetics of EPM under aerobic (a), anaerobic (b), sterilization (c) conditions with 60% moisture, under aerobic conditions with 40% moisture(d) and with
 774 80% moisture(e) in five different agricultural soils (S1 to S5 are defined in Table 1). Values are the means \pm standard error (n=3).

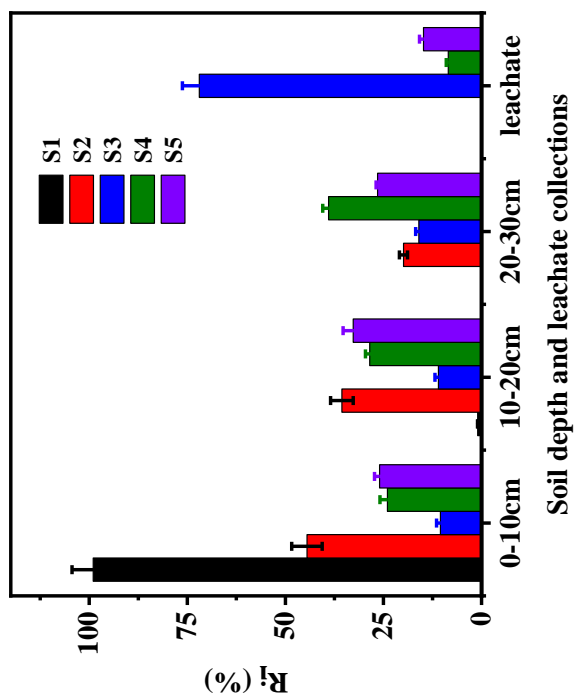


Fig. 3 Distribution of EPM in soil column and leachate of five different agricultural soils (S1 to S5 are defined in [Table 1](#))

775

776

777

778

779